nature physics

ARTICLES

https://doi.org/10.1038/s41567-020-0795-y

Check for updates

Odd elasticity

Colin Scheibner[1,2,8], Anton Souslov[1,3,8], Debarghya Banerjee[4,5], Piotr Surówka[6], William T. M. Irvine[1,2,7] and Vincenzo Vitelli[1,2]✉

A passive solid cannot do work on its surroundings through any quasistatic cycle of deformations. This property places strong constraints on the allowed elastic moduli. In this Article, we show that static elastic moduli altogether absent in passive elasticity can arise from active, non-conservative microscopic interactions. These active moduli enter the antisymmetric (or odd) part of the static elastic modulus tensor and quantify the amount of work extracted along quasistatic strain cycles. In two-dimensional isotropic media, two chiral odd-elastic moduli emerge in addition to the bulk and shear moduli. We discuss microscopic realizations that include networks of Hookean springs augmented with active transverse forces and non-reciprocal active hinges. Using coarse-grained microscopic models, numerical simulations and continuum equations, we uncover phenomena ranging from auxetic behaviour induced by odd moduli to elastic wave propagation in overdamped media enabled by self-sustained active strain cycles. Our work sheds light on the non-Hermitian mechanics of two- and three-dimensional active solids that conserve linear momentum but exhibit a non-reciprocal linear response.

The ability to synthesize systems made of active or driven components has opened new perspectives for materials design[1–7]. Concurrently, significant efforts have been made to expand continuum mechanics to accommodate systems featuring broken spatiotemporal symmetries[8–12], as well as violations of reciprocity relations[13–15] and conservation laws[16–18]. Formulating a continuum theory of active elasticity presents a challenge, because in equilibrium such theories are based on the notion of an elastic potential energy, which is absent in many active systems. In this Article, we examine linear elasticity without making the assumption that an elastic potential energy exists and study the emergent phenomena in two-dimensional (2D) and 3D active solids.

Odd-elastic moduli and quasistatic energy cycles

One of the central assumptions of classical elasticity is that the work needed to quasistatically deform a solid depends only on its initial and final states[19,20]. However, if the microscopic constituents of the solid are active, then the work can be path-dependent. Consider, for example, the network of masses connected by active bonds depicted in Fig. 1a. When the bond elongates or contracts, a gear system rotates the battery-powered propellers to produce transverse forces (Supplementary Video 1). For small strains, the force law is linear in the displacements and is given by

$$\mathbf{F}(r) = (-k\hat{\mathbf{r}} + k^{\mathrm{a}}\hat{\boldsymbol{\phi}})\ \delta r \tag{1}$$

where $\delta r = r - r_0$ is the radial displacement from the equilibrium length r_0, and $\hat{\mathbf{r}}$ and $\hat{\boldsymbol{\phi}}$ are the unit vectors parallel and perpendicular to the bond, respectively (Fig. 1b,c). Equation (1) describes a Hookean spring of spring constant k with an additional chiral, transverse force proportional to k^{a}. When the bond vector is brought through a strain-controlled quasistatic cycle, as shown in Fig. 1d,e, the bond does work given by $W = \oint \mathbf{F}\cdot \mathrm{d}\mathbf{r}$. Because $\nabla \times \mathbf{F} = k^{\mathrm{a}}$ for small displacements, the work done is equal, by Green's theorem, to k^{a} times the area enclosed by the path. The ability to extract work implies that equation (1) does not follow from a potential energy and is necessarily active regardless of the physical realization. Nonetheless, the interaction conserves linear momentum and depends only on the relative positions of the particles.

We now ask 'What is the continuum description of a material built out of many such active components?' Because the energetic state of each microscopic unit has quasistatic path dependence, an elastic potential energy is not well defined. Nonetheless, a stress–strain relation exists and can be linearized for small deformations. This approximation, known as Hooke's law, is captured by the continuum equation $\sigma_{ij}(\mathbf{x}) = C_{ijmn}u_{mn}(\mathbf{x})$, where $u_{mn}(\mathbf{x})$ are the gradients $\partial_m u_n(\mathbf{x})$ of the displacement vector $u_n(\mathbf{x})$ and C_{ijmn} is the elastic modulus tensor. In the absence of an elastic potential energy, the most general linear relationship between stress and displacement gradient for a 2D isotropic solid reads:

$$\begin{pmatrix} \\ \\ \\ \\ \end{pmatrix} = \begin{pmatrix} B & 0 & 0 & 0 \\ A & 0 & 0 & 0 \\ 0 & 0 & \mu & K^{\mathrm{o}} \\ 0 & 0 & -K^{\mathrm{o}} & \mu \end{pmatrix} \begin{pmatrix} \\ \\ \\ \\ \end{pmatrix} \tag{2}$$

irrespective of the details of the microscopic realization (see Methods). In equation (2), we assumed that no stresses arise from solid body rotations of the material.

The notation in equation (2) is a geometric representation of Hooke's law, $\sigma_{ij} = C_{ijmn}u_{mn}$. The displacement gradients on the right-hand side are decomposed into a vector with four independent components: dilation (top entry), rotation (second entry) and the two shear deformations S_1 and S_2 (third and fourth entries, respectively), which are irreducible representations of SO(2). Similarly, the stress vector on the left-hand side of equation (2) is decomposed into pressure (top entry), torque (second entry) and the two shear stresses (third and fourth entries, respectively). We express equation (2) in standard tensor notation in equation (27) of the Methods, and provide an analogous expression for the well-known odd viscosity tensor in the Supplementary Information. Although only two elastic moduli, the bulk modulus B and shear modulus μ, are sufficient

[1]James Franck Institute, The University of Chicago, Chicago, IL, USA. [2]Department of Physics, The University of Chicago, Chicago, IL, USA. [3]Department of Physics, University of Bath, Bath, UK. [4]Max Planck Institute for Dynamics and Self-Organization, Göttingen, Germany. [5]Instituut-Lorentz, Universiteit Leiden, Leiden, The Netherlands. [6]Max Planck Institute for the Physics of Complex Systems, Dresden, Germany. [7]Enrico Fermi Institute, The University of Chicago, Chicago, IL, USA. [8]These authors contributed equally: Colin Scheibner, Anton Souslov. ✉e-mail: vitelli@uchicago.edu

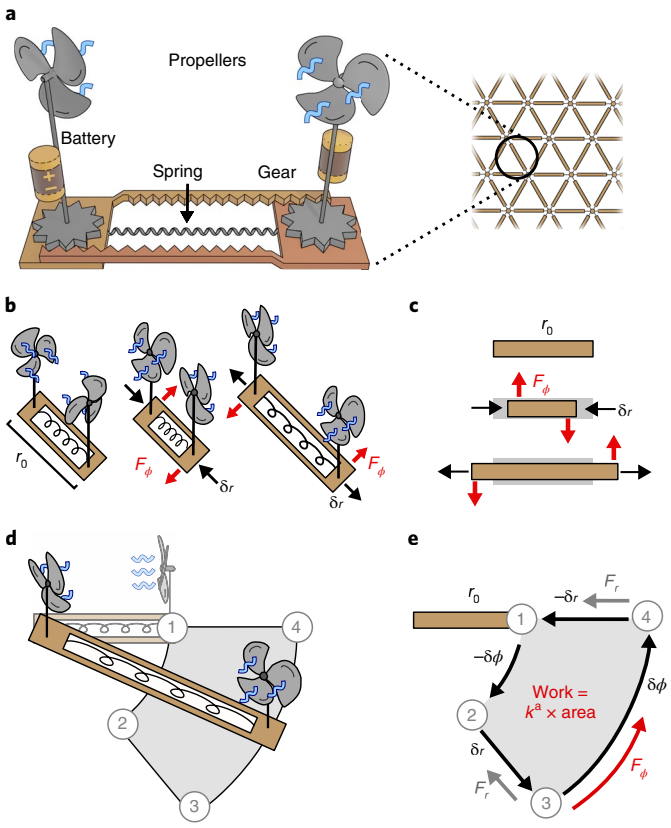

Fig. 1 | Quasistatic energy cycles with non-conservative active bonds. **a**, A mechanical realization of equation (1). Two propellers, mounted on platforms connected by a Hookean spring, are powered by batteries and blow air at a constant rate. As the platforms slide together (or apart), a gear system rotates the propellers, giving rise to transverse forces. An elongated configuration is shown. A triangular lattice built out of such active bonds exhibits odd elasticity. **b**,**c**, The concrete schematic (**b**) and conceptual diagram (**c**) illustrate the linearized force law, given by equation (1). The key feature is an active transverse force (red arrows) proportional to strain (black arrows). (The Hookean spring provides a radial restoring force, not shown.) This interaction is non-reciprocal: extension and compression induce torque, while rotation does not induce or relieve tension. Nonetheless, the interaction conserves linear momentum because the forces on each end of the bond are equal and opposite. **d**,**e**, When the bond is brought on a strain-controlled quasistatic cycle, the work done by the radial forces F_r during legs 2–3 and 4–1 sums to zero. However, the transverse force F_ϕ does work during leg 3–4 that is not compensated elsewhere during the cycle. For small angles $\delta\phi$ and strains $\delta r/r_0$, the work done by the bond on a quasistatic cycle is equal to k^a times the area enclosed.

to describe passive isotropic media, equation (2) features two additional moduli: A and K^o. The modulus A couples compression (and dilation) to an internal torque density (Fig. 2a). By contrast, K^o does not entail a net torque density, but instead implies an antisymmetric shear coupling, which corresponds to a 45° rotation clockwise between the applied shear strain and the resulting shear stress (Fig. 2b). When the microscopic bond in Fig. 1a is placed on a triangular lattice, an analytical coarse-graining reveals $B = 2\mu = \frac{\sqrt{3}}{2}k$ and $A = 2K^o = \frac{\sqrt{3}}{2}k^a$ (see Supplementary Information for details).

The asymmetry of the elastic modulus matrix in equation (2) captures a non-reciprocal, linear response in the continuum, which echoes the non-reciprocal linear response of a single microscopic bond in Fig. 1. Equivalently, moduli A and K^o violate the symmetry of the elastic modulus tensor $C_{ijmn} = C_{mnij}$, which applies whenever the stresses arise from gradients of a free energy $f = \frac{1}{2}C_{ijmn}u_{ij}u_{mn}$ (see Methods). Microscopic units with quasistatic path-dependent work, for example those in Fig. 1, can give rise to an additional contribution to the elastic modulus tensor: $C_{ijmn} = C^e_{ijmn} + C^o_{ijmn}$ with $C^o_{ijmn} = -C^o_{mnij}$, which we refer to as odd elasticity as it is antisymmetric (or odd) under exchange of the first and second pair of indices. The moduli present in C^o_{ijmn} are forbidden by energy conservation, but allowed in active media and metamaterials with non-conservative interactions. For example, the modulus K^o is compatible with broken microscopic time-reversal symmetry in active biological surfaces[8].

Given that C^o_{ijmn} cannot be obtained from a free energy, an odd-elastic solid may be taken through a closed cycle of quasistatic deformations with non-zero total work $\Delta w = \oint C^o_{ijmn}u_{mn}\mathrm{d}u_{ij}$ done by (or on) the material, as anticipated by the microscopic cycles shown in Fig. 1. (See the Methods for a proof.) In Fig. 2c, we apply this general formula to a 2D isotropic solid and illustrate such a cycle using rotations and dilations. The initial and final configurations are identical; hence, zero work is done by the conservative part C^e_{ijmn}. By contrast, the total work done due to the odd contribution C^o_{ijmn} is equal to the modulus A times the area enclosed by the cycle in the space of rotations and dilations. Figure 2d shows an analogous cycle that involves only shear stress and shear strain. During an odd-elastic cycle, the energy generated or lost depends only on the geometry of the path through strain space and not on the strain rate $\dot{u}_{mn}$, in contrast to friction or dissipation, which always lead to energy loss. Other active solids like muscles do work by a different mechanism[21]: as they elongate and contract along the same path in strain space, their active stresses change according to chemical signals instead of strain. By contrast, stresses due to odd elasticity depend on strain alone, and the work extracted depends on the area enclosed in strain space.

Active forces, symmetries and conservation laws

To illustrate how odd elasticity compares to other manifestations of activity in solids[1,3,11,16,22,23], we write the linear active forces F^a_j in the following more general form (see Methods):

$$F^a_j = g_j(\mathbf{u}, \dot{\mathbf{u}}, \nabla\mathbf{u}, \dots) + \partial_i(C_{ijmn}u_{mn} + \eta_{ijmn}\dot{u}_{mn}) \qquad (3)$$

The first term g_j summarizes non-viscoelastic active forces. These forces can be constant or explicitly proportional to displacement u_i, velocity $\dot{u}_i$, strain u_{ij} (refs. [14,24,25]), strain rate $\dot{u}_{ij}$, or to fields other than u_i, such as temperature and electromagnetic fields[2,13], or additional order parameters[18]. This term includes active body forces such as those exhibited by solids formed by self-propelled particles that manifestly violate conservation of linear momentum[26,27]. The second term on the right-hand side of equation (3) captures the forces that result from the divergence of the viscoelastic stress tensor, that is, from two spatial derivatives of displacement and velocity. It is well known that energy sources can renormalize the values of the passive elastic moduli or viscous coefficients that enter the symmetric part of C_{ijmn} or η_{ijmn}, for example negative compressibility[17,28] and viscosity[29]. Activity can also result in odd (or Hall) viscosity, which is the antisymmetric part of the viscosity tensor denoted by $\eta^o_{ijmn} = -\eta^o_{mnij}$ (refs. [9,10,30–32]). However, all the aforementioned effects are physically distinct from odd elasticity, which pertains to the antisymmetric part of C_{ijmn} and is a crucial, but previously absent, piece in the phenomenology of linear active solids.

The distinction between odd and classical elasticity can be understood from the point of view of conservation laws. In classical elasticity, energy conservation is assumed by demanding that an elastic potential exists. Linear and angular momentum conservation, by contrast, is derived from Noether's theorem under the assumption that solid body translations and rotations do not cost elastic potential energy. In lieu of an elastic potential, odd elasticity directly assumes that the elastic stresses must be due to gradients of

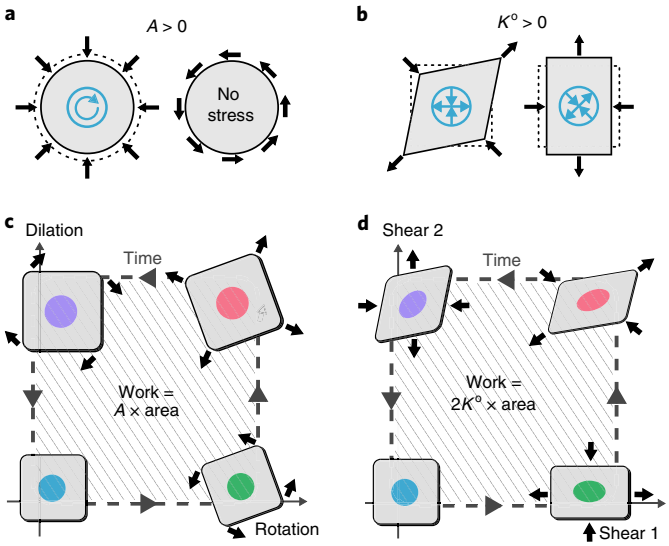

Fig. 2 | Odd-elastic engine cycle. a, The odd modulus A couples compression to an internal torque density, while rotations induce no stresses. The applied strains are represented by black arrows, the undeformed shape by dashed lines and the internal stresses by blue icons. **b**, The odd modulus K^{o} couples the two independent shear deformations. Unlike shear coupling in anisotropic passive solids, the induced stress is always rotated 45° counterclockwise relative to the applied strain. **c**, An odd-elastic material is subjected to a closed cycle in deformation space. First, a counterclockwise rotation is followed by a volumetric strain $\epsilon_{\forall}$, inducing a torque density $A\epsilon_{\forall}$. Next, the object does work $A\epsilon_{\forall}\epsilon_{\theta}$ on its surrounding as it is rotated clockwise through an angle ϵ_{θ}, before being compressed to its original size. The total work done is A times the area enclosed in deformation space: $\epsilon_{\forall}\epsilon_{\theta}$. **d**, An analogous cycle involving only shear stress and shear strain.

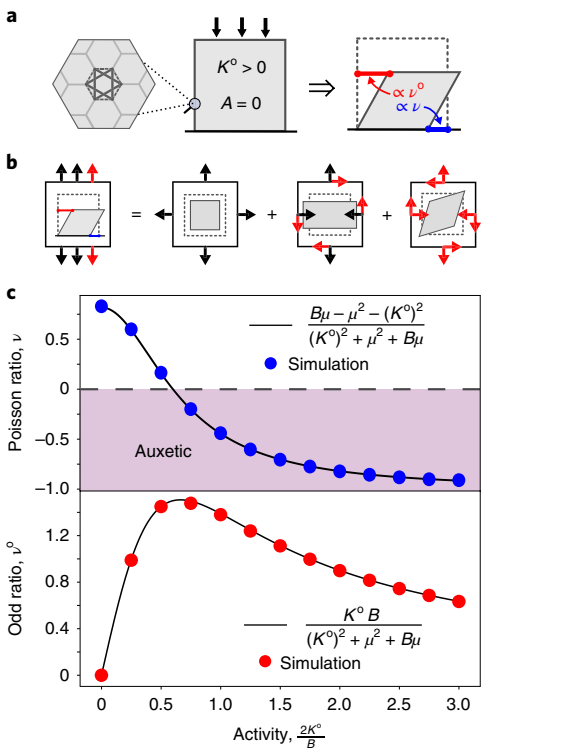

Fig. 3 | Static response in an odd-elastic solid. a, A honeycomb lattice with nearest-neighbour and next-nearest-neighbour odd springs can have $K^{o}>0$ and $A=0$ (and $B, \mu>0$). When subject to uniaxial compression, such a solid responds by both net contraction (proportional to ν (blue)) and horizontal deflection (proportional to ν^{o} (red)). **b**, Force balance in the uniaxial compression, shown schematically. Net strain can be decomposed into compression and shear in two directions. The resulting boundary stresses (arrows) cancel pressure on the top and bottom surfaces and maintain no stress on the sides. Black arrows show the response in the absence of odd elasticity and red arrows show the stresses due to K^{o}. **c**, Analytical calculations for the odd and Poisson's ratios with numerical validation. Simulations are performed using the honeycomb lattice (see Supplementary Information).

displacement, which is sufficient to ensure linear momentum conservation, but not angular momentum conservation (see Methods). As a consequence, an odd-elastic solid can experience an internal torque density even when solid body rotations do not induce stress. For example, in the microscopic model shown in Fig. 1, compression and elongation result in microscopic torques, which then leads to the elastic modulus A in the continuum limit.

Given the appearance of additional elastic moduli, for example A and K^{o} in equation (2), a natural question is how to control their relative values by microscopic design. For example, are there microscopic building blocks for odd elasticity that, in contrast to Fig. 1, conserve angular momentum? In the Supplementary Information, we show that such a unit must involve non-pairwise interactions. Extended Data Fig. 1a shows an example built from motorized hinges that exert angular tensions to widen or contract each angle of a honeycomb plaquette. Crucially, each motor is designed to exert an angular tension proportional to the angular strain of its counterclockwise neighbour only. This is captured by the equation

$$T_i = -\kappa\delta\theta_i - \kappa^{a}\delta\theta_{i-1} \tag{4}$$

where T_i and $\delta\theta_i$ are, respectively, the angular tension and displacement of the ith vertex, κ provides passive bond bending stiffness and κ^{a} provides the crucial non-conservative, non-reciprocal response. Like the model in Fig. 1, equation (4) does not follow from a potential because the active plaquette may be brought through a quasi-static cycle that extracts energy, as shown in Extended Data Fig. 1b. Moreover, linear momentum is conserved and the forces only depend on the relative positions of the particles. However, given that each angular motor, by definition, exerts equal and opposite torques on its two constituent edges, the total angular momentum is conserved, in contrast to the active bonds in Fig. 1. As a result, the modulus A, and any entry in the second row of the matrix in equation (2), must be zero for a material built out of these plaquettes. We note that the microscopic models in both Fig. 1 and Extended Data Fig. 1 will also give contributions to the antisymmetric parts of the viscosity tensor $\eta^{o}_{ijmn} = -\eta^{o}_{mnij}$ in a viscoelastic solid when δr and $\delta\theta_i$ in equations (1) and (4) are replaced by $\delta\dot{r}$ and $\delta\dot{\theta}_i$, respectively (see Supplementary Information). Furthermore, both the microscopic models are chiral. In the Supplementary Information, we show that 2D odd-elastic solids must be chiral provided that they are isotropic, but anisotropic ones need not be.

The concept of odd elasticity extends naturally to three dimensions. In analogy to equation (2), a full classification of odd elasticity in 3D is obtained by decomposing the strain tensor using irreducible representations of SO(3) (see Supplementary Information). The elastic modulus tensor displays up to 36 moduli that are not present in standard elasticity because they cannot be derived from an elastic potential, and these moduli yield up to four independent elastic energy cycles. A 3D odd-elastic solid must necessarily be anisotropic[33,34], and the elastic modulus tensor in 3D is always achiral, irrespective of odd elasticity. We note that odd elasticity cannot exist in solids

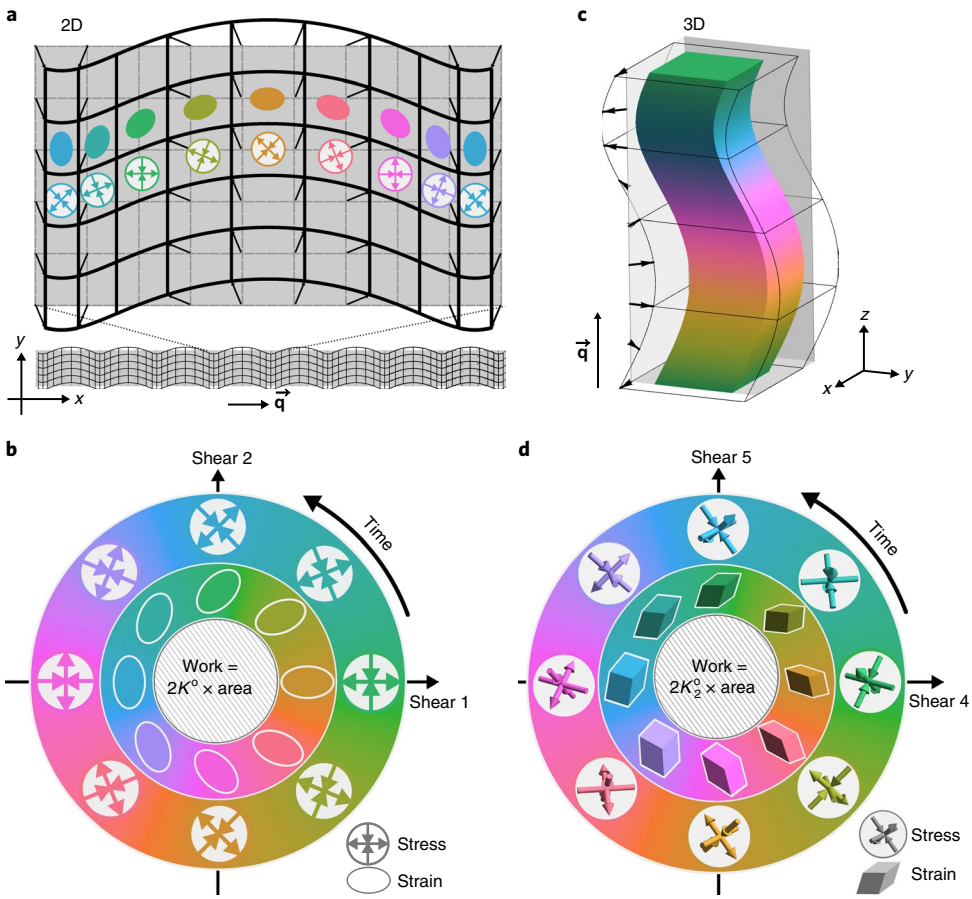

Fig. 4 | Odd-elastic waves. a, Real-space profile of an overdamped odd-elastic wave travelling in the positive $\hat{x}$ direction (for $K^{o} \gg A, B, \mu$). The light grey background shows the undeformed material; the wave deforms the background grid into the thick black mesh. The ellipses illustrate the shear strain in a material patch and the disk-confined arrows represent the local shear stress. **b**, If a single material patch is tracked in time, the strain in the material traces out a circle in shear space. This circular trajectory encloses an area in strain space such that internal energy balances dissipative losses. The other essential ingredient for wave propagation is that stress and strain inside each patch are 90° out of phase (colour represents time) (Supplementary Video 2). **c**, A 3D odd-elastic wave travelling in a viscoelastic medium. The background grey represents the undeformed solid, and the coloured interior and thin black frame represent a snapshot of the wave. Black arrows represent the displacement field and trace out a helix in the $\hat{z}$ direction. **d**, The cycle traced out by a single patch of material in strain space. The wave is powered by an odd-elastic engine cycle in the space of shear 4 and shear 5, which are unique to three dimensions (see Supplementary Information).

embedded in one dimension because the elastic modulus tensor is a scalar and hence cannot be antisymmetric.

Odd elastostatics

In the presence of odd elasticity, even the most familiar elastic phenomena appear in a new guise. Consider, as an example, Poisson's ratio $\nu \equiv -\frac{u_{xx}}{u_{yy}}$, which is the ratio between horizontal strain u_{xx} and vertical strain u_{yy} under uniaxial compression along $\hat{y}$. In the absence of odd elasticity, Poisson's ratio can be made negative by altering the bulk and shear moduli B and μ, for example via the geometry of the microscopic structures[35–38] or energy flux[28]. Here, we focus on the effect of odd elasticity, which does not alter B and μ, but instead introduces additional elastic moduli.

Figure 3a shows the uniaxial compression of an odd-elastic material having K^{o}, B, $\mu > 0$ and $A = 0$. In the Supplementary Information, we show that as $\left|\frac{2K^{o}}{B}\right|$ increases, the Poisson's ratio of a stable odd-elastic solid approaches $\nu = -1$, the auxetic limit of stable passive solids. Moreover, an additional response, not observed in passive elasticity, emerges, where the odd solid exhibits a horizontal deflection of the top surface with respect to the bottom surface, which we quantify via the odd ratio, $\nu^{0} \equiv -\frac{u_{yx}}{2u_{yy}}$. Whereas in passive isotropic solids the odd ratio is zero due to left–right symmetry, the odd shear coupling K^{o} manifestly breaks chiral symmetry and thus allows for deflection. In Fig. 3c, we plot analytical predictions for ν and ν^{o} as solid black lines. To validate our analytical results, we simulate a honeycomb lattice with nearest-neighbour and next-nearest-neighbour active bonds for which $A = 0$. Using an analytic coarse-graining procedure (see Supplementary Information), we obtain the values of K^{o}, μ, B and A from the microscopic spring constants. The measured Poisson's ratio, plotted in Fig. 3c, agrees well with the prediction of the continuum theory without any fitting parameters.

Odd elastodynamics

Now we turn to odd elastodynamics. In passive materials, elastic waves cannot propagate when either (1) the bulk and shear moduli are vanishingly small, $B = \mu = 0$, or (2) the solid is overdamped. By contrast, odd-elastic solids exhibit waves that propagate without any attenuation when both of these conditions are met because activity provides the energy to overcome dissipation in each wave cycle. Figure 4a shows a snapshot of a plane wave

travelling to the right in an overdamped solid in which $K^o \gg A, B, \mu$ (Supplementary Videos 2 and 3). The overdamped equation of motion is $\Gamma \dot{u}_j = \partial_i \sigma_{ij}$, where Γ is a friction coefficient with a substrate. (The momentum-conserving case of viscous damping, in which the dissipation is due to the relative velocity of solid particles, is treated in the Supplementary Information.) The coloured ellipses in Fig. 4a (cf. Fig. 2d) represent the strain in regions bounded by the thick, black lines, with the corresponding shear stresses shown in the row underneath. In Fig. 4b, we plot the stress and strain of a single deformed square as a function of time (indicated by colour) in the space of shear S_1 and S_2. Figure 4c,d shows the analogous plots for a wave travelling in a 3D odd-elastic medium (see Supplementary Information for a detailed treatment).

Figure 4b illustrates two crucial features of waves in an overdamped odd-elastic solid. First, stress and strain are 90° out of phase due to the antisymmetric shear coupling K^o. Thus, stress and strain in an overdamped odd-elastic wave mimic the phase delay between strain and velocity that enables wave propagation in underdamped passive solids. Second, the trajectory of the wave in strain space traces out a circle. This circle indicates the emergence of an autonomous, self-sustaining elastic engine cycle, in which the system converts internal energy into mechanical work to offset dissipative losses (Fig. 2c). The speed of the wave, calculated in the Supplementary Information, can be intuited using a simple argument based on the balance of activity and dissipation. For a wave of amplitude R and wave number q, an infinitesimal piece of material traces out a circle in strain space of radius qR, and so the energy injected due to activity is $2K^o \times \text{area} = 2\pi K^o (qR)^2$. The energy loss due to dissipation in a single cycle is $\Gamma \times \text{velocity} \times \text{distance travelled} = 2\pi\Gamma\omega R^2$. Balancing the energy injected with the energy dissipated, one obtains the dispersion $\omega = K^o q^2/\Gamma$, and therefore the group velocity $\mathrm{d}\omega/\mathrm{d}q = 2K^o q/\Gamma$.

More generally, when B, μ, A and K^o are all non-zero, the equation of motion reads

$$-i\omega\Gamma \begin{pmatrix} u_\parallel \\ u_\perp \end{pmatrix} = -q^2 \begin{pmatrix} B+\mu & K^o \\ -K^o - A & \mu \end{pmatrix} \begin{pmatrix} u_\parallel \\ u_\perp \end{pmatrix} \qquad (5)$$

where $u_\parallel$ is the longitudinal displacement and $u_\perp$ is the transverse displacement. To obtain the spectrum, we solve the secular equation corresponding to equation (5) (see Supplementary Information for the full expression). The active moduli enter the spectrum through the quantity $J = K^o(K^o + A)$. The qualitative behaviour of the solid changes depending on whether J is above or below the threshold value $(B/2)^2$. For large J, waves propagate but attenuate exponentially with a rate proportional to $B/2 + \mu$. When J is smaller than the threshold, there is a sharp cutoff below which the real part of the spectrum vanishes, and no waves propagate. The phase diagram in Fig. 5a summarizes the dynamic behaviour of isotropic odd-elastic solids, with the transition highlighted in red.

The matrix on the right-hand side of equation (5) times $-q^2$ is known as the dynamical matrix. Because odd elasticity arises from linear, non-reciprocal interactions, the dynamical matrix is non-Hermitian. As illustrated in Fig. 5b and Supplementary Video 4, the onset of odd-elastic waves displays characteristic features of non-Hermitian systems. In the absence of activity (circle symbol), the two eigenmodes are longitudinal and transverse. As activity increases, the eigenvectors are no longer orthogonal, and at the threshold $|k^a/k| = \frac{1}{\sqrt{3}}$, the eigenvectors become co-linear (star symbol). The singularity caused by the degeneracy of the eigenvectors is a hallmark feature of non-Hermitian dynamics and is known as an exceptional point[39,40]. Above the exceptional point (square symbol), odd-elastic waves propagate with circular polarization, tracing out a spiral in shear space due to attenuation. In the limit $|k^a/k| \gg 1$, the waves become self-sustaining and the spiral expands into an ellipse.

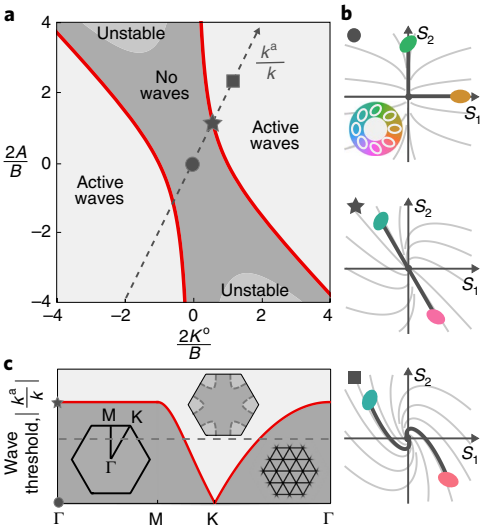

Fig. 5 | Exceptional points and non-Hermitian elastodynamics. a, Phase diagram for waves in an overdamped odd-elastic solid. The red curves represent the boundary outside of which active waves can be sustained. **c**, A cut (ΓMKΓ) through the space of wavevectors (first Brillioun zone) of a triangular lattice with generalized Hookean springs. The microscopic activity in the springs is characterized by the ratio $\left|\frac{k^a}{k}\right|$ between odd spring constant k^a and conservative spring constant k. The threshold for active waves varies across the Brillioun zone, with the elastic limit describing the region near Γ. The middle inset shows the regions of the Brillouin zone (light grey) in which waves propagate (for $\left|\frac{k^a}{k}\right|$ corresponding to the horizontal dashed line). **b**, The eigenmodes for three relative values of the elastic moduli, showing trajectories in shear space (S_1 and S_2, Fig. 4). At zero activity (circle symbol), the modes correspond to longitudinal and transverse waves, whose eigenvectors are orthogonal in S_1–S_2 space. At the exceptional point (star symbol), the eigenmodes become co-linear. Above the exceptional point (square symbol), the eigenmodes acquire a circular polarization, performing a spiral through simultaneous rotation and attenuation in strain space. See Supplementary Video 4.

To understand the spectrum at shorter wavelengths, a microscopic structure must be specified. In Fig. 5c, we consider an unbounded triangular lattice of springs with conservative spring constant k and odd spring constant k^a. Analytic coarse-graining shows that this microscopic realization corresponds to a position (set by k^a/k) on the dashed line in Fig. 5a. Elasticity describes the dynamics in the neighbourhood of Γ, and the ΓMKΓ cut in Fig. 5c shows how the wave propagation threshold varies depending on the wavevector within the Brillouin zone. At zero activity, the spectrum of the triangular lattice is pierced by Dirac points at K and Γ. The exceptional points at K split into exceptional rings that flow outward. When $|k^a/k| = \frac{1}{\sqrt{3}}$ the exceptional rings merge along the line ΓK and the bands open. The middle inset of Fig. 5c highlights the regions in the Brillouin zone (light grey) for which waves can propagate when, as an example, $\left|\frac{k^a}{k}\right|$ is given by the horizontal dashed line. The surprising feature is the existence of waves at short length scales well below the critical value in the continuum theory of Fig. 5a.

Future work will explore applications of our findings to biomechanical systems[8,41–43], kinematics of systems with transverse interactions such as gyroscopes or vortex lattices[44], viscoelastic quantum Hall states[45] and active metamaterials[14,46] functioning as emergent soft robots that harvest energy, transmit it using odd mechanical waves and perform work at designated sites. In addition, odd elasticity provides an alternative approach to design energy-absorbing materials that exploit quasistatic cycles instead of rate-dependent deformations.

Online content

Any methods, additional references, Nature Research reporting summaries, source data, extended data, supplementary information, acknowledgements, peer review information; details of author contributions and competing interests; and statements of data and code availability are available at https://doi.org/10.1038/s41567-020-0795-y.

Received: 26 March 2019; Accepted: 10 January 2020;
Published online: 2 March 2020

References

1. van Zuiden, B. C., Paulose, J., Irvine, W. T. M., Bartolo, D. & Vitelli, V. Spatiotemporal order and emergent edge currents in active spinner materials. *Proc. Natl Acad. Sci. USA* **113**, 12919–12924 (2016).
2. Lakes, R. Giant enhancement in effective piezoelectric sensitivity by pyroelectric coupling. *Europhys. Lett.* **98**, 47001 (2012).
3. Lau, A. W. C., Hoffman, B. D., Davies, A., Crocker, J. C. & Lubensky, T. C. Microrheology, stress fluctuations, and active behavior of living cells. *Phys. Rev. Lett.* **91**, 198101 (2003).
4. Thompson, J. M. T. 'Paradoxical' mechanics under fluid flow. *Nature* **296**, 135–137 (1982).
5. Cui, H. et al. Three-dimensional printing of piezoelectric materials with designed anisotropy and directional response. *Nat. Mater.* **18**, 234–241 (2019).
6. Polygerinos, P. et al. Soft robotics: review of fluid-driven intrinsically soft devices; manufacturing, sensing, control, and applications in human–robot interaction. *Adv. Eng. Mater.* **19**, 1700016 (2017).
7. Roche, E. T. et al. A bioinspired soft actuated material. *Adv. Mater.* **26**, 1200–1206 (2014).
8. Salbreux, G. & Jülicher, F. Mechanics of active surfaces. *Phys. Rev. E* **96**, 032404 (2017).
9. Soni, V. et al. The odd free surface flows of a colloidal chiral fluid. *Nat. Phys.* **15**, 1188–1194 (2019).
10. Banerjee, D., Souslov, A., Abanov, A. G. & Vitelli, V. Odd viscosity in chiral active fluids. *Nat. Commun.* **8**, 1573 (2017).
11. Maitra, A. & Ramaswamy, S. Oriented active solids. *Phys. Rev. Lett.* **123**, 238001 (2019).
12. Souslov, A., van Zuiden, B. C., Bartolo, D. & Vitelli, V. Topological sound in active-liquid metamaterials. *Nat. Phys.* **13**, 1091–1094 (2017).
13. Faust, D. & Lakes, R. S. Reciprocity failure in piezoelectric polymer composite. *Phys. Scripta* **90**, 085807 (2015).
14. Brandenbourger, M., Locsin, X., Lerner, E. & Coulais, C. Non-reciprocal robotic metamaterials. *Nat. Commun.* **10**, 4608 (2019).
15. Coulais, C., Sounas, D. & Alù, A. Static non-reciprocity in mechanical metamaterials. *Nature* **542**, 461–464 (2017).
16. Marchetti, M. C. et al. Hydrodynamics of soft active matter. *Rev. Mod. Phys.* **85**, 1143–1189 (2013).
17. Lakes, R. Stable singular or negative stiffness systems in the presence of energy flux. *Philos. Mag. Lett.* **92**, 226–234 (2012).
18. Prost, J., Jülicher, F. & Joanny, J. Active gel physics. *Nat. Phys.* **11**, 111–117 (2015).
19. Landau, L. et al. *Theory of Elasticity* (Elsevier, 1986).
20. Lakes, R. *Viscoelastic Materials* (Cambridge Univ. Press, 2009).
21. Caruel, M. & Truskinovsky, L. Physics of muscle contraction. *Rep. Progr. Phys.* **81**, 036602 (2018).
22. Hemingway, E. J. et al. Active viscoelastic matter: from bacterial drag reduction to turbulent solids. *Phys. Rev. Lett.* **114**, 098302 (2015).
23. Murrell, M., Oakes, P. W., Lenz, M. & Gardel, M. L. Forcing cells into shape: the mechanics of actomyosin contractility. *Nat. Rev. Mol. Cell Biol.* **16**, 486–498 (2015).
24. Beatus, T., Tlusty, T. & Bar-Ziv, R. Phonons in a one-dimensional microfluidic crystal. *Nat. Phys.* **2**, 743–748 (2006).
25. Beatus, T., Bar-Ziv, R. & Tlusty, T. Anomalous microfluidic phonons induced by the interplay of hydrodynamic screening and incompressibility. *Phys. Rev. Lett.* **99**, 124502 (2007).
26. Protière, S., Couder, Y., Fort, E. & Boudaoud, A. The self-organization of capillary wave sources. *J. Phys. Condens. Matter* **17**, S3529–S3535 (2005).
27. Lieber, S. I., Hendershott, M. C., Pattanaporkratana, A. & Maclennan, J. E. Self-organization of bouncing oil drops: two-dimensional lattices and spinning clusters. *Phys. Rev. E* **75**, 056308 (2007).
28. Lakes, R. & Wojciechowski, K. W. Negative compressibility, negative Poisson's ratio, and stability. *Phys. Status Solidi B* **245**, 545–551 (2008).
29. Starr, V. P. *Physics of Negative Viscosity Phenomena* (McGraw-Hill, 1968).
30. De Groot, S. R. *Non-equilibrium Thermodynamics* (North-Holland, 1962).
31. Avron, J. E. Odd viscosity. *J. Stat. Phys.* **92**, 543–557 (1998).
32. Wiegmann, P. & Abanov, A. G. Anomalous hydrodynamics of two-dimensional vortex fluids. *Phys. Rev. Lett.* **113**, 034501 (2014).
33. Day, W. A. Restrictions on relaxation functions in linear viscoelasticity. *Q. J. Mech. Appl. Math.* **24**, 487–497 (1971).
34. Rogers, T. G. & Pipkin, A. C. Asymmetric relaxation and compliance matrices in linear viscoelasticity. *Z. Angew. Math. Phys.* **14**, 334–343 (1963).
35. Lakes, R. Foam structures with a negative Poisson's ratio. *Science* **235**, 1038–1040 (1987).
36. Greaves, G. N., Greer, A. L., Lakes, R. S. & Rouxel, T. Poisson's ratio and modern materials. *Nat. Mater.* **10**, 823–837 (2011).
37. Bertoldi, K., Reis, P. M., Willshaw, S. & Mullin, T. Negative Poisson's ratio behavior induced by an elastic instability. *Adv. Mater.* **22**, 361–366 (2010).
38. Spadoni, A. & Ruzzene, M. Elasto-static micropolar behavior of a chiral auxetic lattice. *J. Mech. Phys. Solids* **60**, 156–171 (2012).
39. Bender, C. M. & Boettcher, S. Real spectra in non-Hermitian Hamiltonians having *PT* symmetry. *Phys. Rev. Lett.* **80**, 5243–5246 (1998).
40. Heiss, W. The physics of exceptional points. *J. Phys. A* **45**, 444016 (2012).
41. Needleman, D. & Dogic, Z. Active matter at the interface between materials science and cell biology. *Nat. Rev. Mater.* **2**, 17048 (2017).
42. Bi, D., Yang, X., Marchetti, M. C. & Manning, M. L. Motility-driven glass and jamming transitions in biological tissues. *Phys. Rev. X* **6**, 021011 (2016).
43. Moshe, M., Bowick, M. J. & Marchetti, M. C. Geometric frustration and solid–solid transitions in model 2D tissue. *Phys. Rev. Lett.* **120**, 268105 (2018).
44. Nash, L. M. et al. Topological mechanics of gyroscopic metamaterials. *Proc. Natl Acad. Sci. USA* **112**, 14495–14500 (2015).
45. Offertaler, B. & Bradlyn, B. Viscoelastic response of quantum Hall fluids in a tilted field. *Phys. Rev. B* **99**, 035427 (2019).
46. Woodhouse, F. G., Ronellenfitsch, H. & Dunkel, J. Autonomous actuation of zero modes in mechanical networks far from equilibrium. *Phys. Rev. Lett.* **121**, 178001 (2018).

Methods

Elastic energy and symmetries of the elastic modulus tensor. The standard theory of elasticity begins with the postulation of an elastic free energy density f (for example, ref. [19]). The free energy density is a function of the displacement field u_i, which is the order parameter arising from the translational degrees of freedom of the microscopic constituents. The requirement that the elastic free energy be invariant under translations of the solid implies $\frac{\partial f}{\partial u_i} = 0$, so the free energy is only a function of gradients of u_i. In the limit of long-wavelength deformations, the lowest-order gradient $u_{ij} = \partial_i u_j$ dominates. Mechanical stability implies $\frac{\partial f}{\partial u_{ij}}|_{u_{ij}=0} = 0$, so the lowest-order term in strain must be quadratic. To linear order, the distances between points change only due to changes in the symmetrized displacement gradients $u^s_{ij} \equiv \frac{1}{2}(\partial_i u_j + \partial_j u_i)$. Therefore, u^s_{ij} defines the linear strain tensor, and the elastic free energy may be written as

$$f = \frac{1}{2} K_{ijmn} u^s_{ij} u^s_{mn} \tag{6}$$

where K_{ijmn} is a constant rank-4 tensor.

The stress tensor is given by

$$\sigma^{eq}_{ij} = \frac{\partial f}{\partial u^s_{ij}} = \frac{1}{2}(K_{ijmn} + K_{mnij}) u^s_{mn} \tag{7}$$

Thus, we obtain the constitutive relation $\sigma^{eq}_{ij} = C_{ijmn} u^s_{mn}$, where C_{ijmn} is known as the elastic modulus tensor. From equation (7) we see that

$$C_{ijmn} = \frac{1}{2}(K_{ijmn} + K_{mnij}) = C_{mnij} \tag{8}$$

Therefore, if a solid medium obeys a linear constitutive relation that follows from a free energy, then the elastic modulus tensor must obey the major symmetry $C_{ijmn} = C_{mnij}$. Note that the definition $\sigma^{eq}_{ij} \equiv \partial f / \partial u^s_{ij}$ implies that the stress is symmetric, $\sigma^{eq}_{ij} = \sigma^{eq}_{ji}$ (because u^s_{ij} is symmetric). In turn, this means that the non-active solid has no internal torques (evaluated as $\sigma^{eq}_{ij}\epsilon_{ij} = 0$, where ϵ_{ij} is the 2D Levi-Civita symbol).

To consider an odd-elastic component $C^o_{ijmn} = -C^o_{mnij}$, we cannot start in the usual way from an elastic free energy. Instead, we begin from the constitutive relations directly: $\sigma_{ij} = C_{ijmn} u^s_{mn}$. If, unlike equation (7), the constitutive relations are not derived from an elastic free energy density, then an odd-elastic component can exist. Materials with non-zero C^o_{ijmn} violate Maxwell–Betti reciprocity, that is, mechanical reciprocity in their static response. Unlike ref. [15], the non-reciprocity is present already in the linear response and relies on activity rather than nonlinearities in the microscopic structure. Furthermore, the non-reciprocity due to C^o_{ijmn} is distinct from that observed in piezoelectrics[2,13], which concerns the electromagnetic degrees of freedom, and from viscous effects, which depend on strain rate[20]. See Supplementary Section I for more details.

Classification of 2D elastic moduli. We now examine the basic features of linear elasticity in the absence of an elastic potential energy. To begin, we suppose a solid body undergoes a deformation such that a point originally located at position $\mathbf{x}$ (having components x_i) ends up at location $X_i(\mathbf{x})$. We define the displacement vector field for the solid to be $u_i(\mathbf{x}) \equiv X_i(\mathbf{x}) - x_i$, and define the displacement gradient tensor to be $u_{ij}(\mathbf{x}) \equiv \partial_i u_j(\mathbf{x})$ (that is, u_{ij} is related to the deformation gradient tensor $\Lambda_{ij} \equiv \partial X_i(\mathbf{x})/\partial x_j$ via $u_{ij} = \Lambda_{ij} - \delta_{ij}$, where δ_{ij} is the Kronecker-δ). Note that, to linear order, u_{ij} plays the role of an unsymmetrized elastic strain tensor, which under the assumption of deformation dependence (see below) can be symmetrized in the usual way. The continuum version of Hooke's law postulates that if the displacement gradients are sufficiently small, the stress field $\sigma_{ij}(\mathbf{x})$ induced in a solid due to the displacement gradients is given by

$$\sigma_{ij}(\mathbf{x}) = C_{ijmn} u_{mn}(\mathbf{x}) \tag{9}$$

where C_{ijmn} is known as the elastic modulus tensor. In what follows, we assume that the material is homogeneous, which implies that C_{ijmn} is constant in space. The components of C_{ijmn} are known as elastic moduli, and they are the coefficients of proportionality between stress and strain that characterize the elastic behaviour of a solid.

As we now show, basic assumptions about the interactions within the solid, such as conservation of angular momentum and conservation of energy, guarantee symmetries of the elastic modulus tensor. For convenience, we work in two dimensions (see Supplementary Information for the 3D case) and we introduce the following basis for 2×2 matrices:

$$\tau^0 = \begin{pmatrix} 1 & 0 \\ 0 & 1 \end{pmatrix} \tag{10}$$

$$\tau^1 = \begin{pmatrix} 0 & -1 \\ 1 & 0 \end{pmatrix} \tag{11}$$

$$\tau^2 = \begin{pmatrix} 1 & 0 \\ 0 & -1 \end{pmatrix} \tag{12}$$

$$\tau^3 = \begin{pmatrix} 0 & 1 \\ 1 & 0 \end{pmatrix} \tag{13}$$

In this basis, we define

$$u^0(\mathbf{x}) = \tau^0_{ij} u_{ij}(\mathbf{x}) \text{ Dilation} \tag{14}$$

$$u^1(\mathbf{x}) = \tau^1_{ij} u_{ij}(\mathbf{x}) \text{ Rotation} \tag{15}$$

$$u^2(\mathbf{x}) = \tau^2_{ij} u_{ij}(\mathbf{x}) \text{ Shear strain 1} \tag{16}$$

$$u^3(\mathbf{x}) = \tau^3_{ij} u_{ij}(\mathbf{x}) \text{ Shear strain 2} \tag{17}$$

These four independent components define the full displacement gradient tensor and can be interpreted as follows. The quantity u^0 measures the local, isotropic dilation of the solid. A dilation corresponds to change in area without change in shape or orientation. By contrast, u^1 measures the local rotation, which corresponds to change in orientation without change in shape or area. Under transformations of 2D space, u^0 has the symmetry of a scalar and u^1 has the symmetry of a pseudo-scalar. The two components u^2 and u^3 define the shear strain, which corresponds to change in shape without change in area or orientation. Under rotations of 2D space, u^2 and u^3 both behave as bivectors, that is, double-headed arrows. The space spanned by τ^2 and τ^3 is precisely that of symmetric traceless tensors. Specifically, u^2 measures shear strain with extension along the x axis and contraction along the y axis (or vice versa), which we dub shear 1 for convenience. On the other hand, u^3 measures shear 2, which has the axis of extension rotated 45° counterclockwise with respect to shear 1. Note that two independent shear vectors (in addition to compression and rotation) are needed to form a complete basis for arbitrary deformations.

We choose the same basis for the stress tensor:

$$\sigma^0(\mathbf{x}) = \tau^0_{ij} \sigma_{ij}(\mathbf{x}) \text{ Pressure} \tag{18}$$

$$\sigma^1(\mathbf{x}) = \tau^1_{ij} \sigma_{ij}(\mathbf{x}) \text{ Torque density} \tag{19}$$

$$\sigma^2(\mathbf{x}) = \tau^2_{ij} \sigma_{ij}(\mathbf{x}) \text{ Shear stress 1} \tag{20}$$

$$\sigma^3(\mathbf{x}) = \tau^3_{ij} \sigma_{ij}(\mathbf{x}) \text{ Shear stress 2} \tag{21}$$

The physical interpretations of these stresses are analogous to those for the strains. The quantity σ^0 is the (negative) of the isotropic pressure. The component σ^1 captures the antisymmetric part of the stress, that is, the torque density. The two remaining components, σ^2 and σ^3, correspond to shear stresses.

In this notation, we express the elastic modulus tensor as a 4×4 matrix $C^{\alpha\beta} = \frac{1}{2}\tau^\beta_{ij} C_{ijmn} \tau^\alpha_{mn}$. Then equation (9) becomes

$$\begin{pmatrix} \sigma^0(\mathbf{x}) \\ \sigma^1(\mathbf{x}) \\ \sigma^2(\mathbf{x}) \\ \sigma^3(\mathbf{x}) \end{pmatrix} = 2 \begin{pmatrix} C^{00} & C^{01} & C^{02} & C^{03} \\ C^{10} & C^{11} & C^{12} & C^{13} \\ C^{20} & C^{21} & C^{22} & C^{23} \\ C^{30} & C^{31} & C^{32} & C^{33} \end{pmatrix} \begin{pmatrix} u^0(\mathbf{x}) \\ u^1(\mathbf{x}) \\ u^2(\mathbf{x}) \\ u^3(\mathbf{x}) \end{pmatrix} \tag{22}$$

Here, we review certain physical symmetries and conservation laws that constrain the form of $C^{\alpha\beta}$. The assumptions are stated independently and may be read in any order.

Deformation dependence. A solid body rotation of a material does not change the distance between points within that material (that is, the metric). Therefore, one generally assumes that solid body rotations do not induce stress, because stresses should only emerge if the object is deformed, not merely reoriented. This assumption is equivalent to the minor symmetry $C_{ijmn} = C_{ijnm}$ or, in the notation of equation (22), $C^{\alpha 1} = 0$ for all α. Note that, in our derivation, we use the displacement gradient tensor $u_{ij} \equiv \partial_i u_j$ instead of the linear symmetrized strain $u^s_{ij} \equiv \frac{1}{2}(\partial_i u_j + \partial_j u_i)$ or the full nonlinear strain tensor $u^{nl}_{ij} \equiv \frac{1}{2}(\Lambda_{ik}\Lambda_{kj} - \delta_{ij})$. The full tensor u^{nl}_{ij} is rotationally invariant at all orders, and at linear order reduces to u^s_{ij}. If C_{ijmn} has the minor symmetry $C_{ijmn} = C_{ijnm}$, then the product $C_{ijmn}u_{mn}$ is the same whether or not u_{mn} is symmetrized. We choose to work with the displacement gradient tensor u_{mn} (that is, unsymmetrized strain) to be explicit about the assumption of non-coupling to rotation. Under deformation dependence alone, the elastic modulus tensor contains 12 independent moduli.

Isotropy. Isotropy implies that the elastic modulus tensor remains unchanged through a rotation of the coordinate system. A passive rotation of the coordinate system through an angle θ maps $C^{\alpha\beta} \mapsto R^{\alpha\gamma}(\theta) C^{\gamma\sigma} R^{\beta\sigma}(\theta)$, where

$$R^{\gamma\sigma}(\theta)=\begin{pmatrix}1&0&0&0\\0&1&0&0\\0&0&\cos(2\theta)&\sin(2\theta)\\0&0&-\sin(2\theta)&\cos(2\theta)\end{pmatrix} \tag{23}$$

The requirement of isotropy can be restated as $C^{\alpha\beta}=R^{\alpha\gamma}(\theta)C^{\gamma\sigma}R^{\beta\sigma}(\theta)$ for all θ. Hence, under the assumption of isotropy alone, the most general form of the elastic modulus tensor is

$$C^{\alpha\beta}=2\begin{pmatrix}C^{00}&C^{01}&0&0\\C^{10}&C^{11}&0&0\\0&0&C^{22}&C^{23}\\0&0&-C^{23}&C^{22}\end{pmatrix} \tag{24}$$

Therefore, under isotropy alone, the elastic modulus tensor has six independent moduli.

Conservation of energy. Energy is fundamentally a conserved quantity. However, the constituents of a solid may have internal or external sources of energy that can be integrated out, resulting in phenomena that ostensibly violate energy conservation. In section 'Elastic engine cycle', we show that an elastic modulus tensor is compatible with an elastic potential if and only if $C_{ijmn}=C_{mnij}$. In the notation of equation (22), the condition for energy conservation is $C^{\alpha\beta}=C^{\beta\alpha}$. Under conservation of energy alone, the elastic modulus tensor contains 10 independent moduli.

Conservation of angular momentum. A material conserves angular momentum if it has no internal sources of torque. In this case, one requires that $\sigma_{ij}=\sigma_{ji}$ or, equivalently, $\sigma^{1}(\mathbf{x})=0$. To impose this constraint, one has to impose the left minor symmetry for the elastic modulus tensor $C_{ijmn}=C_{jimn}$ or, in the notation of equation (22), $C^{1\alpha}=0$ for all α. A medium with internal torques (generated, for example, by interactions with a substrate or internal spinning parts, see Supplementary Information) may violate the symmetry of the stress tensor and therefore violate the left minor symmetry of the elastic modulus tensor. As with energy, angular momentum is a fundamentally conserved quantitiy, so any gain or loss of angular momentum must come from an internal or external angular momentum sink that has been integrated out of the analysis. Under conservation of angular momentum alone, the elastic modulus tensor has 12 independent moduli.

If deformation dependence is the only assumption present, then $C^{\alpha\beta}$ has 12 independent components. In the standard theory of linear elasticity with energy conservation, the number of independent components is reduced to 6. Note that, when deformation dependence and energy conservation are both assumed, conservation of angular momentum is automatically implied because the left minor symmetry required for conservation of angular momentum is guaranteed by the right minor symmetry of deformation dependence in combination with the major symmetry associated with energy conservation. If one further assumes isotropy, the form of the elastic modulus tensor is restricted to have two independent components B and μ:

$$C^{\alpha\beta}=2\begin{pmatrix}B&0&0&0\\0&0&0&0\\0&0&\mu&0\\0&0&0&\mu\end{pmatrix} \tag{25}$$

Here, B is the familiar bulk modulus, which is the proportionality constant between compression and pressure. The quantity μ is the shear modulus, which is the proportionality constant between shear stress and shear strain.

For equation (2), we retain only deformation dependence and isotropy. We assume deformation dependence because stress only arises in the solids we consider as a result of relative displacements (that is, changes in the material's metric). Note that isotropy is not a strict requirement, and many crystalline solids have anisotropic elastic modulus tensors. However, we consider only the isotropic case for simplicity. In this work we study odd elasticity, which arises when we lift the assumption of an elastic potential energy (that is, conservation of energy). Assuming only isotropy and deformation dependence, the most general form of the elastic modulus tensor is

$$C^{\alpha\beta}=2\begin{pmatrix}B&0&0&0\\A&0&0&0\\0&0&\mu&K^{o}\\0&0&-K^{o}&\mu\end{pmatrix} \tag{26}$$

In this case, there are two new moduli: A and K^{o}. As described in the main text, A couples compression to internal torque density. The modulus K^{o}, like the shear modulus μ, is a proportionality constant between shear stress and shear strain. However, K^{o} mixes the two independent shears in an antisymmetric way.

Note that energy conservation is independent of angular momentum conservation. We consider both cases: case (i), in which angular momentum is conserved and the solid has no internal torque density (that is, $A=0$), and case (ii), in which internal torques are present (that is, $A\neq 0$). Even if $A=0$, the modulus K^{o} can be non-zero. Hence, the existence of odd elasticity is not contingent on the presence of antisymmetric stress (or, equivalently, local torques).

In index notation, the most general form of the elastic modulus tensor from equation (26) is

$$\begin{aligned}C_{ijmn} &= B\delta_{ij}\delta_{mn}+\mu(\delta_{in}\delta_{jm}+\delta_{im}\delta_{jn}-\delta_{ij}\delta_{mn})\\ &+ K^{o}E_{ijmn}-A\epsilon_{ij}\delta_{mn}\end{aligned} \tag{27}$$

where

$$E_{ijmn}\equiv\frac{1}{2}(\epsilon_{im}\delta_{jn}+\epsilon_{in}\delta_{jm}+\epsilon_{jm}\delta_{in}+\epsilon_{jn}\delta_{im}) \tag{28}$$

Odd elasticity in a general continuum framework for active solids. Odd elasticity is not a generic term for activity in solids, but rather a well-defined physical mechanism that generates active forces in solids or in other systems in which a generalized elasticity can be defined without using an elastic potential. In Supplementary Section I, we provide a detailed comparison between odd elasticity and other phenomena in solid mechanics. This section provides a justification for equation (3) and illustrates how odd elasticity fits into a larger continuum framework of active solids. A continuum theory of a solid describes the dynamics of the displacement field u_i along with a set of fields χ_α that represent additional degrees of freedom such as temperature, chemical concentration, electromagnetic fields, a nematic director, a microrotation field and so on (explicit examples are provided in Supplementary Section I). We take the fields χ_α to be independent in that there is no constitutive relation allowing one field to be statically determined by the others.

The dynamics of the displacement field will be governed by the force density F_i, which we assume can be expanded in powers of χ_α and u_i (and their gradients) about a steady state or equilibrium value. We split the forces into two contributions:

$$F_i=F_i^{\chi}+F_i^{\mathrm{d}} \tag{29}$$

F_i^{χ} are the forces that are proportional to χ_α or their derivatives. For example, in a piezoelectric solid with electric field E_k and piezoelectric tensor e_{ijk}, there is a contribution to the stress of the form $\sigma_{ij}=e_{ijk}E_k$, yielding a force term $f_j=e_{ijk}\partial_i E_k$ (refs. [2,13]). In the case of active gels, the stress acquires a contribution of the form $\sigma_{ij}=\alpha Q_{ij}$, where Q_{ij} is the nematic order parameter and α is a constant[18]. See Supplementary Section I for more details and references.

F_i^{d} captures all forces that are proportional to u_i or its derivatives. We assume the u_i and their gradients are small, so we retain only linear terms up to two derivatives in space and one derivative in time. The F_j^{d} may then be written as

$$\begin{aligned}F_i^{\mathrm{d}} = &\ (A_{ij}+B_{ij}\partial_t)u_j+(D_{ijk}+H_{ijk}\partial_t)\partial_j u_k\\ &+(C_{ijmn}+\eta_{ijmn}\partial_t)\partial_j u_{mn}\end{aligned} \tag{30}$$

The first two terms, proportional to A_{ij} and B_{ij}, physically represent, for example, pinning and substrate drag. The term proportional to D_{ijk} represents linear momentum exchange with a substrate and has been considered in refs. [14,24,25] (see Supplementary Information) and is distinct from elasticity because the force is proportional to strain instead of gradients of strain. The final two terms represent linear viscoelasticity. The tensor η_{ijmn} is known as the viscosity tensor and relates stress to strain rate. The tensor C_{ijmn} is the elastic modulus tensor and relates stress directly to strain. All the tensor coefficients in equation (30) could in principle be functions of the χ_α. For example, in mechanocaloric solids and shape memory alloys, the elastic moduli are temperature-dependent (see Supplementary Information). Furthermore, it has been shown that η_{ijmn} can acquire a non-zero antisymmetric part $\eta^{o}_{ijmn}=-\eta^{o}_{mnij}$, which is known as odd (or Hall) viscosity. All these effects are distinct from odd elasticity because odd elasticity refers to a non-zero antisymmetric part of C_{ijmn}, not merely a renormalization of the symmetric part of C_{ijmn}.

The quantity F_i^{a} in equation (3) in the main text illustrates many of the ways in which activity can manifest in continuum theories of solids. The term g_j includes the forces F_i^{χ} and the first four terms of equation (30). The second term in equation (3) highlights explicitly the role of viscoelasticity. Our contribution in this work is to highlight that activity can introduce an antisymmetric part of the elastic modulus tensor and to explore its phenomenology and microscopic origins.

Elastic engine cycle. In this section, we show that an elastic modulus tensor follows from an elastic potential if and only if $C_{ijmn}=C_{mnij}$. Furthermore, we justify the formulae in Fig. 2c,d, which relate the work done by an odd-elastic solid when taken on a (quasistatic) deformation cycle to the area enclosed in strain space.

To begin, we represent C_{ijmn} as a 4×4 matrix $C_{\alpha\beta}$ (see section 'Classification of 2D elastic moduli') and write $C_{\alpha\beta}=C^{e}_{\alpha\beta}+C^{o}_{\alpha\beta}$, where $C^{e}_{\alpha\beta}=C^{e}_{\beta\alpha}$ is even (symmetric) and $C^{o}_{\alpha\beta}=-C^{o}_{\beta\alpha}$ is odd (antisymmetric). Using this notation, the

work per unit area done on a solid in a quasistatic, infinitesimal deformation is given by

$$\mathrm{d}w = \sigma_{ij}\mathrm{d}u_{ij} \tag{31}$$

$$= \frac{1}{2}\sigma^{\alpha}\mathrm{d}u^{\alpha} \tag{32}$$

$$= \frac{1}{2}C_{\alpha\beta}u^{\alpha}\mathrm{d}u^{\beta} \tag{33}$$

If we take a piece of material through a path of strains that returns to the initial configuration, then the total work per unit area done on the material is

$$w = \frac{1}{2}\oint C_{\alpha\beta}u^{\alpha}\mathrm{d}u^{\beta} \tag{34}$$

$$= \frac{1}{2}\oint C^{\mathrm{e}}_{\alpha\beta}u^{\alpha}\mathrm{d}u^{\beta} + \frac{1}{2}\oint C^{\mathrm{o}}_{\alpha\beta}u^{\alpha}\mathrm{d}u^{\beta} \tag{35}$$

Integration by parts yields

$$\oint C^{\mathrm{e}}_{\alpha\beta}u^{\alpha}\mathrm{d}u^{\beta} = -\oint C^{\mathrm{e}}_{\alpha\beta}u^{\beta}\mathrm{d}u^{\alpha} \text{ Integration by parts} \tag{36}$$

$$= -\oint C^{\mathrm{e}}_{\beta\alpha}u^{\alpha}\mathrm{d}u^{\beta} \text{ Relabel indices} \tag{37}$$

$$= -\oint C^{\mathrm{e}}_{\alpha\beta}u^{\alpha}\mathrm{d}u^{\beta} \;\; C^{\mathrm{e}}_{\alpha\beta} = C^{\mathrm{e}}_{\beta\alpha} \tag{38}$$

Consequently, $\frac{1}{2}\oint C^{\mathrm{e}}_{\alpha\beta}u^{\alpha}\mathrm{d}u^{\beta} = 0$. This can also be seen directly because $C^{\mathrm{e}}_{\alpha\beta}$ arises from a potential energy (section 'Elastic energy and symmetries of the elastic modulus tensor'): because the potential energy depends only on the configuration and not on the deformation path, the energy has to be the same at the beginning and end of the closed cycle. Therefore, the contribution to net work must be zero. We now evaluate $\frac{1}{2}\oint C^{\mathrm{o}}_{\alpha\beta}u^{\alpha}\mathrm{d}u^{\beta}$. For an isotropic solid, the antisymmetric part $C^{\mathrm{o}}_{\alpha\beta}$ takes the form

$$C^{\mathrm{o}}_{\alpha\beta} = \begin{pmatrix} 0 & -A & 0 & 0 \\ A & 0 & 0 & 0 \\ 0 & 0 & 0 & 2K^{\mathrm{o}} \\ 0 & 0 & -2K^{\mathrm{o}} & 0 \end{pmatrix} \tag{39}$$

In the case of a more general solid, such as one that violates isotropy or deformation dependence (see section 'Classification of 2D elastic moduli'), we can still choose an orthonormal basis in shear space such that $C^{\mathrm{o}}_{\alpha\beta}$ takes the form

$$C^{\mathrm{o}}_{\alpha\beta} = \begin{pmatrix} 0 & G & 0 & 0 \\ -G & 0 & 0 & 0 \\ 0 & 0 & 0 & H \\ 0 & 0 & -H & 0 \end{pmatrix} \tag{40}$$

Let $\{g_0, g_1, h_0, h_1\}$ be the basis vectors in this basis. For an isotropic solid, the basis vectors are simply

$$g_0 = \begin{pmatrix} 1 \\ 0 \\ 0 \\ 0 \end{pmatrix} \quad g_1 = \begin{pmatrix} 0 \\ 1 \\ 0 \\ 0 \end{pmatrix} \tag{41}$$

$$h_0 = \begin{pmatrix} 0 \\ 0 \\ 1 \\ 0 \end{pmatrix} \quad h_1 = \begin{pmatrix} 0 \\ 0 \\ 0 \\ 1 \end{pmatrix} \tag{42}$$

The total work per unit area done on the solid can be computed by projecting the path through 4D strain space onto paths in the 2D subspaces of g_i and h_i:

$$w = \frac{G}{2}\oint \epsilon_{ij}g_j\mathrm{d}g_i + \frac{H}{2}\oint \epsilon_{ij}h_j\mathrm{d}h_i \tag{43}$$

where in this case the i and j indices run over 0 and 1. Examples of these paths for a 2D isotropic odd-elastic solid are illustrated in Fig. 2c,d. Let A_g be the region enclosed by the g_i path and A_h be the region enclosed by the h_i path. Application of Stokes' theorem then gives

$$w = G\int_{A_g}\mathrm{d}^2g + H\int_{A_h}\mathrm{d}^2h \tag{44}$$

$$= G\ \mathrm{area}(A_g) + H\ \mathrm{area}(A_h) \tag{45}$$

To conclude, if $C^{\mathrm{o}}_{\alpha\beta}$ is non-zero, then a closed deformation cycle with $w \neq 0$ can always be found by choosing a path in strain space that encloses a non-zero area in the g_i or h_i planes. Importantly, if there exists a cycle such that $w \neq 0$, then C_{ijmn} does not follow from an elastic potential energy. However, if the major symmetry $C_{ijmn} = C_{mnij}$ holds, then the odd-elastic component is zero ($C^{\mathrm{o}}_{\alpha\beta} = 0$), so $w = 0$ and no work is done on or by the material during a closed cycle due to elastic stresses. Here, we have presented the proof in two dimensions, but the same approach holds in three dimensions, as explained in Supplementary Section G.

Data availability

The data represented in Fig. 3c are available as Source Data Fig. 3. All other data that support the plots within this paper and other findings of this study are available from the corresponding author upon reasonable request.

Code availability

The code used to perform and analyse the numerics in this work is available from the corresponding author upon reasonable request.

Acknowledgements

V.V. was supported by the Complex Dynamics and Systems Program of the Army Research Office under grant no. W911NF-19-1-0268. V.V., A.S. and W.T.M.I. acknowledge primary support through the Chicago MRSEC, funded by the NSF through grant no. DMR-1420709. A.S. acknowledges the support of the Engineering and Physical Sciences Research Council (EPSRC) through New Investigator Award no. EP/T000961/1. C.S. was supported by the National Science Foundation Graduate Research Fellowship under grant no. 1746045. W.T.M.I. acknowledges support from NSF EFRI NewLAW grant no. 1741685 and NSF DMR 1905974. D.B. was supported by FOM and NWO. P.S. was supported by the Deutsche Forschungsgemeinschaft via the Leibniz Program. We thank R. Lakes, F. Jülicher and G. Salbreux for their critical readings of the manuscript.

Author contributions

V.V. initiated the research. C.S., A.S., W.T.M.I. and V.V. prepared the manuscript. All authors conducted the research, revised the manuscript and contributed to discussions.

Competing interests

The authors declare no competing interests.

Additional information

Extended data is available for this paper at https://doi.org/10.1038/s41567-020-0795-y.

Supplementary information is available for this paper at https://doi.org/10.1038/s41567-020-0795-y.

Correspondence and requests for materials should be addressed to V.V.

Peer review statement *Nature Physics* thanks Roderic Lakes and the other, anonymous, reviewer(s) for their contribution to the peer review of this work.

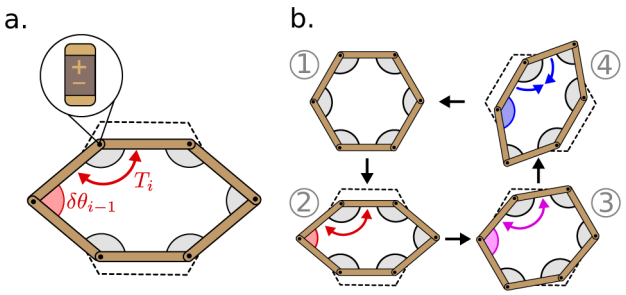

Extended Data Fig. 1 | Active hinge model. a. A honeycomb plaquette with active hinges at each vertex. Each hinge exerts an angular tension T_i based on the angular strain $\delta\theta_{i-1}$ of its counterclockwise neighbor. **b**. A quasistatic, strain-controlled cycle in which the plaquette does work on its surroundings.